1   **SARS-CoV-2 vaccination induces neutralizing antibodies against pandemic and pre-**

2   **emergent SARS-related coronaviruses in monkeys**

3

4   Kevin O. Saunders[1,2,3,4,#], Esther Lee[1,5], Robert Parks[1,5], David R. Martinez[6], Dapeng Li[1,5],

5   Haiyan Chen[1,5], Robert J. Edwards[1,5], Sophie Gobeil[1,5], Maggie Barr[1,5], Katayoun Mansouri[1,5], S.

6   Munir Alam[1,5], Laura L. Sutherland[1,5], Fangping Cai[1,5], Aja M. Sanzone[1,5], Madison Berry[1,5],

7   Kartik Manne[1,5], Anyway B. Kapingidza[1,5], Mihai Azoitei[1,5], Longping V. Tse[6], Trevor D. Scobey[6],

8   Rachel L. Spreng[1,5], R. Wes Rountree[1,5], C. Todd DeMarco[1,5], Thomas N. Denny[1,5], Christopher

9   W. Woods[1,5,7], Elizabeth W. Petzold[7], Thomas H. Oguin III[1,5], Gregory D. Sempowski[1,5],

10   Matthew Gagne[8], Daniel C. Douek[8], Mark A. Tomai[9], Christopher B. Fox[10], Robert Seder[8], Kevin

11   Wiehe[1,5], Drew Weissman[11], Norbert Pardi[11], Priyamvada Acharya[1,5], Hanne Andersen[12], Mark

12   G. Lewis[12], Ian N. Moore[13], David C. Montefiori[1,2], Ralph S. Baric[6], Barton F. Haynes[1,3,5,#]

13

14   [1]Duke Human Vaccine Institute, Duke University School of Medicine, Durham, NC 27710, USA

15   [2]Department of Surgery, Duke University, Durham, NC 27710, USA

16   [3]Department of Immunology, Duke University School of Medicine, Durham, NC 27710, USA

17   [4]Department of Molecular Genetics and Microbiology, Duke University School of Medicine,

18   Durham, NC 27710, USA

19   [5]Department of Medicine, Duke University School of Medicine, Durham, NC 27710, USA

20   [6]Department of Epidemiology, University of North Carolina at Chapel Hill, Chapel Hill, NC

21   27599, USA

22   [7]Center for Applied Genomics and Precision Medicine, Duke University Medical Center,

23   Durham, NC 27710, USA

24   [8]Vaccine Research Center, National Institute of Allergy and Infectious Diseases (NIAID), NIH,

25   Bethesda, MD 20892, USA

26   [9]Corporate Research Materials Lab, 3M Company, St. Paul, MN 55144, USA.

27   [10]Infectious Disease Research Institute, Seattle, WA 98102, USA

28   [11]Department of Medicine, University of Pennsylvania, Philadelphia, PA 19104, USA

29   [12]BIOQUAL, Rockville, MD 20850, USA

30   [13]Infectious Disease Pathogenesis Section, Comparative Medicine Branch, National Institute of

31   Allergy and Infectious Diseases, National Institutes of Health, Bethesda, MD 20892, USA.

32

33   [#]Correspondence: barton.haynes@duke.edu (B.F.H.) and kevin.saunders@duke.edu (K.O.S.)

34 **SUMMARY (150 words)**

35 Betacoronaviruses (betaCoVs) caused the severe acute respiratory syndrome (SARS) and

36 Middle East Respiratory Syndrome (MERS) outbreaks, and now the SARS-CoV-2 pandemic.

37 Vaccines that elicit protective immune responses against SARS-CoV-2 and betaCoVs

38 circulating in animals have the potential to prevent future betaCoV pandemics. Here, we show

39 that immunization of macaques with a multimeric SARS-CoV-2 receptor binding domain (RBD)

40 nanoparticle adjuvanted with 3M-052-Alum elicited cross-neutralizing antibody responses

41 against SARS-CoV-1, SARS-CoV-2, batCoVs and the UK B.1.1.7 SARS-CoV-2 mutant virus.

42 Nanoparticle vaccination resulted in a SARS-CoV-2 reciprocal geometric mean neutralization

43 titer of 47,216, and robust protection against SARS-CoV-2 in macaque upper and lower

44 respiratory tracts. Importantly, nucleoside-modified mRNA encoding a stabilized transmembrane

45 spike or monomeric RBD protein also induced SARS-CoV-1 and batCoV cross-neutralizing

46 antibodies, albeit at lower titers. These results demonstrate current mRNA vaccines may

47 provide some protection from future zoonotic betaCoV outbreaks, and provide a platform for

48 further development of pan-betaCoV nanoparticle vaccines.

49

50 **MAIN**

51 The emergence of three betacoronavirus (BetaCoV) outbreaks over the last 18 years

52 necessitates the development of countermeasures that can prevent future pandemics [1-4].

53 SARS-CoV-1 and SARS-CoV-2 (betaCoV group 2b) and MERS (betaCoV group 2c) emerged

54 from cross-species transmission events where humans were infected with bat or camel CoVs [5-9].

55 In particular, betaCoVs that are genetically similar to SARS-CoV-1 and SARS-CoV-2 and bind

56 to the human ACE2 receptor for virus entry circulate in civets, bats, and Malayan pangolins [5,6,10-12].

57 Thus, SARS-related animal coronaviruses represent betaCoVs that can be transmitted to

58 humans. Neutralizing antibodies can prevent or treat betaCoV infection and represent potential

59 countermeasures against current human betaCoVs and pre-emergent viruses [13-22]. Cross-

60 neutralizing antibodies capable of neutralizing multiple betaCoVs, have been isolated from

61 SARS-CoV-1 infected humans [13,23,24], providing proof-of-concept for development of betaCoV

62 vaccines against group 2b *Sarbecoviruses* [25]. A critical target of cross-neutralizing antibodies is

63 the receptor binding domain (RBD) [22,23,25]. RBD immunogenicity can be augmented by arraying

64 multiple copies of it on nanoparticles, mimicking multimeric virus-like particles [26-30]. Vaccine

65 induction of cross-neutralizing antibodies has been reported in *in vitro* neutralization assays

66 against CoV pseudoviruses in mice [29,30]. However, it is unknown whether spike vaccination of

67 primates can elicit cross-neutralizing betaCoV antibodies against SARS-CoV-1, bat betaCoVs,

68 or against SARS-CoV-2 escape viruses. Here, we demonstrate the ability of a SARS-CoV-2

69 RBD 24-mer subunit nanoparticle vaccine—produced with an easily modifiable sortase-ferritin

70 platform[31]—to elicit in monkeys potent cross-neutralizing antibodies against SARS-CoV-1,

71 SARS-CoV-2, SARS-CoV-2 variant B.1.1.7, as well as SARS-related bat betaCoVs. RBD

72 nanoparticle vaccination protected monkeys against SARS-CoV-2 after respiratory challenge.

73 Lastly, we show lipid nanoparticle-encapsulated Spike mRNA vaccines similar to those in

74 clinical use elicit cross-neutralizing CoV antibodies, albeit at lower titers.

75

76 We and others have demonstrated the SARS-CoV-2 RBD has an epitope to which broadly

77 cross-reactive neutralizing antibodies can bind [13,24,32], and the DH1047 RBD antibody cross-

78 neutralizes SARS-CoV-1, CoV-2 and bat CoVs[24].To focus the immune response on cross-

79 reactive neutralizing epitopes on betaCoVs, we designed a 24-mer SARS-CoV-2 RBD-ferritin

80 nanoparticle vaccine. The RBD nanoparticle was constructed by first expressing recombinant

81 SARS-CoV-2 RBD with a C-terminal sortase A donor sequence. Next, we expressed the 24-

82 subunit, self-assembling protein nanoparticle *Helicobacter pylori* ferritin with an N-terminal

83 sortase A acceptor sequence [31]. The RBD and *H. pylori* ferritin nanoparticle were conjugated

84 together by a sortase A reaction (**Fig. 1a, Extended data Fig. 1**) [31]. Analytical size exclusion

85 chromatography and negative stain electron microscopy confirmed that RBD was conjugated to

86 the surface of the ferritin nanoparticle (**Fig. 1a**, **Extended data Fig. 1b,c).** The RBD sortase A

87 conjugated nanoparticle (RBD-scNP) bound to human ACE2, the receptor for SARS-CoV-2, and

88 to potently neutralizing RBD antibodies DH1041, DH1042, DH1043, DH1044, and DH1045 [24]

89 (**Fig. 1b**). The epitopes of these antibodies are focused on the receptor binding motif within the

90 RBD [24]. Cross-neutralizing antibody DH1047 also bound to the RBD-scNP (**Fig. 1b**). The RBD

91 scNP lacked binding to SARS-CoV-2 spike antibodies that bound outside of the RBD (**Fig. 1b**).

92

93 To assess immunogenicity of the RBD scNP, we immunized five cynomolgus macaques three

94 times intramuscularly four weeks apart (**Fig. 1c**). Immunogenicity of the protein was adjuvanted

95 with the TLR7/8 agonist 3M-052 absorbed to alum [33]. After a single immunization, all five

96 macaques generated binding IgG antibodies against SARS-CoV-2 RBD and stabilized Spike

97 ectodomain (S-2P) (**Fig. 1d**). Boosting once maximally increased plasma SARS-CoV-2 RBD

98 and S-2P-specific IgG antibody titers (**Fig. 1d**). ACE2 competitive binding assays demonstrated

99 the presence of antibodies against the ACE2 binding site within the receptor binding domain.

100 Plasma antibodies blocked the ACE2 binding site on SARS-CoV-2 S-2P by 52% after one

101 immunization and 100% after two immunizations (**Fig. 1e**). Similarly, plasma antibodies blocked

102 the binding of ACE2-binding site-focused, RBD neutralizing antibody DH1041, although to a

103 lesser degree than ACE2 (**Fig. 1e**). Vaccine induction of neutralizing antibodies was assessed

104 against a SARS-CoV-2 pseudovirus with an aspartic acid to glycine substitution at position 614

105 (D614G)[34]. Two RBD scNP immunizations induced potent serum neutralizing antibodies (**Fig.**

106 **1f-h**). The fifty percent inhibitory reciprocal serum dilution (ID50) neutralization titers ranged

107 from 21,292 to 162,603 (**Fig. 1g**). In cynomolgus macaques, serum neutralization titers against

108 SARS-CoV-2 D614G pseudovirus elicited by RBD-scNP immunization were significantly higher

109 than titers elicited by stabilized transmembrane (TM) Spike (S-2P) lipid-encapsulated

110 nucleoside-modified mRNA (mRNA-LNP) immunization that is analogous to the immunogen and

111 vaccine platform in the Moderna and Pfizer/BioNTech COVID-19 vaccines (**Fig. 1i,** $P<0.01$

112   Exact Wilcoxon test, n=5)[35,36]. The group geometric mean ID50, measured as reciprocal serum

113   dilution, for the macaques immunized with RBD-ScNP was 47,216 compared to 6,469 for

114   mRNA-LNP immunized macaques. When compared to natural infection, RBD-scNP vaccination

115   elicited ID50 neutralization titers higher than those elicited in humans with SARS-CoV-2

116   symptomatic infection, asymptomatic infection, or infection requiring hospitalization (**Fig. 1j**).

117   Thus, RBD-scNP vaccination elicits significantly higher neutralizing titers compared to current

118   vaccine platforms and natural infection.

119

120   The new SARS-CoV-2 variant B.1.1.7 is widespread in the United Kingdom (UK) and is

121   spreading globally[37,38]. Moreover, the B.1.1.7 variant has been suggested to have higher

122   infectivity and has mutations in the receptor binding domain that may limit neutralization efficacy

123   of RBD-specific antibodies [37,38]. Therefore, we tested the serum from the RBD-scNP-vaccinated

124   macaques against a pseudovirus with B.1.1.7 spike. The macaque serum potently neutralized a

125   pseudovirus bearing the Spike from the B.1.1.7 variant of SARS-CoV-2 (**Fig. 2a,b**). Similarly,

126   neutralizing antibodies elicited by mRNA-LNP encoding the stabilized TM spike neutralized the

127   B.1.1.7 variant of SARS-CoV-2 equally as well the D614G variant of SARS-CoV-2, albeit at

128   titers below those observed with RBD-scNP immunization (**Fig. 2a,b**). Thus, the potentially

129   more transmissible B.1.1.7 variant of SARS-CoV-2 was equally susceptible to vaccine-induced

130   neutralizing antibodies as the SARS-CoV-2 D614G variant. Additionally, we determined RBD-

131   scNP and S-2P mRNA-LNP immune plasma IgG binding to S ectodomain spike proteins

132   containing mutations observed in strains circulating in Danish minks, as well as B1.351, P.1,

133   and B.1.1.7 SARS-CoV-2 strains [38-40]. As a control, we tested ACE2 receptor and SARS-CoV-2

134   cross-neutralizing antibody DH1047 binding to each spike mutant. The presence of D614G

135   increased binding to spike by ACE2 and RBD cross-reactive antibody DH1047 (**Fig. 2c,d**).

136   Similarly, plasma IgG from S-2P mRNA-LNP-immunized macaques and RBD-scNP-immunized

137   macaques exhibited increased binding to spike in the presence of D614G (**Fig. 2c,d**). The

138 addition of mutations from mink strains of SARS-CoV-2, the South African B1.351, Brazilian P.1

139 strain, and UK B.1.1.7 strains did not change binding magnitude for DH1047 nor macaque

140 plasma IgG (**Fig. 2c,d**). However, the addition of these mutations slightly increased ACE2

141 binding compared to D614G alone (**Fig. 2c**). Next we tested binding to recombinant RBD

142 monomers with and without the K417N, E484K, and N501Y mutations present in the B1.351

143 variant. ACE2 binding was decreased by K417N and increased by N501Y, while the RBD with

144 all three mutations showed no change in ACE2 binding (**Fig. 2e**). RBD neutralizing antibody

145 DH1041 is focused on the ACE2 binding site, and was knocked out by the E484K change (**Fig.**

146 **2e**). Importantly, the binding to SARS-CoV-2 RBD for cross-reactive antibody DH1047 was

147 unchanged to RBDs with E484K or other mutations (**Fig. 2f**). Also, RBD-scNP-vaccinated

148 macaque plasma IgG and S-2P mRNA-LNP-immunized macaque plasma IgG were unaffected

149 by the RBD mutations (**Fig. 2e,f**). [41] Thus, RBD-scNP and mRNA-LNP-induced RBD binding

150 antibodies were not sensitive to spike mutations present in neutralization-resistant UK, South

151 Africa or Brazil SARS-CoV-2 variants.

152

153 While SARS-CoV-2 wild-type and variant neutralization remain a priority for halting the current

154 pandemic, additional SARS-related CoVs that circulate in humans and animals remain a threat

155 for future outbreaks [42-44]. Therefore, we examined neutralization of SARS-CoV-1, SARS-related

156 batCoV-WIV-1 and SARS-related batCoV-SHC014 by immune serum from vaccinated

157 macaques[6,10,43,44]. After two immunizations, RBD-scNP, S-2P mRNA-LNP, and the RBD

158 monomer mRNA-LNP elicited neutralizing antibodies against SARS-CoV-1, batCoV-WIV-1, and

159 batCoV-SHC014 (**Fig. 3a, Extended data Fig. 2**). Neutralization was more potent for

160 replication-competent SARS-CoV-2 virus compared to the other three SARS-related viruses

161 (**Fig. 3a, Extended data Fig. 2**). Among the three immunogens, RBD-scNP elicited the highest

162 neutralization titers and mRNA-LNP expressing monomer RBD elicited the lowest neutralization

163 titers (**Fig. 3a, Extended data Fig. 2**). Also, RBD-scNP immunization elicited cross-reactive IgG

164   binding against SARS-CoV-2, SARS-CoV-1, batCoV-RaTG13, batCoV-SHC014, pangolin CoV-

165   GXP4L Spike proteins (**Fig. 3c** and **Extended data Figs. 3a,c**). RBD-scNP immune plasma IgG

166   did not bind the S ectodomain of four endemic human CoVs, nor did it bind MERS-CoV S

167   ectodomain (**Extended data figs. 3a,c**). The lack of binding by plasma IgG to these latter five S

168   ectodomains was consistent with RBD sequence divergence among groups 1, 2a, 2b and 2c

169   coronaviruses (**Fig. 3e and Extended data figs. 4-6**). Nonetheless, the SARS-CoV-2 spike

170   induced cross-reactive antibodies against multiple group 2b SARS-related betaCoVs, with the

171   highest titers induced by RBD-scNP.

172

173   The immune sera from RBD-scNP-immunized exhibited a similar cross-neutralizing profile as

174   the cross-neutralizing antibody DH1047. DH1047 binds with <0.02 nM affinity to monomeric

175   SARS-CoV-2 RBD (**Extended data fig. 3b**), and bound the RBD-scNP (**Fig. 1b**). DH1047

176   protects against SARS-CoV-2 infection in macaques and batCoV-WIV-1 infection in mice[24]; thus

177   the DH1047 epitope is a principal betacoronavirus (CoV) cross-neutralizing antibody target for

178   vaccination. The cross-reactive DH1047 epitope is adjacent to the N-terminus of the receptor

179   binding motif distinguishing it from dominant RBM-focused neutralizing antibodies such as

180   DH1041[24] (**Fig. 3d**). Antibodies targeting near the DH1047 epitope would be predicted to be

181   cross-reactive with group 2b betaCoVs given the high sequence conservation present in and

182   immediately proximal to the DH1047 epitope (**Fig. 3e**). Comparison of RBD sequences showed

183   them to be relatively conserved within betaCoV group 2b, but minimally conserved between

184   groups 2b and 2c (**Fig. 3f and Extended data figs. 4-6**). To examine whether RBD-scNP-

185   induced antibodies bound near the DH1047 epitope, we assessed plasma antibody blocking of

186   DH1047 binding to SARS-CoV-2 S-2P ectodomain. Plasma from all RBD-scNP immunized

187   macaques blocked the binding of ACE2 and DH1047 to SARS-CoV-2 S-2P ectodomain (**Fig. 3g**

188   **and Extended data fig. 3d**). Since DH1047-blocking plasma antibodies could be SARS-CoV-2-

189   specific, we also examined plasma IgG blocking of DH1047 binding to batCoV-SHC014. Similar

190   to SARS-CoV-2 S binding, RBD-scNP plasma also blocked DH1047 binding to batCoV-SHC014

191   (**Fig. 3g**). While 96% of COVID-19 patients made antibodies that blocked ACE2 as a dominant

192   RBD response, only 31% made antibodies that blocked the cross-reactive antibody, DH1047

193   (**Fig. 3h**). Thus, in natural SARS-CoV-2 infection the cross-reactive DH1047 IgG blocking

194   response is subdominant, and RBD-scNP vaccination focused antibody responses to this

195   subdominant cross-reactive neutralizing epitope.

196

197   Finally, to determine whether vaccination elicited coronavirus protective immunity, we

198   challenged RBD scNP-vaccinated monkeys with 10^5 plaque forming units of SARS-CoV-2 virus

199   (**Fig 4a**). To assess virus replication in the upper and lower respiratory tract, E or N sgRNA was

200   quantified in fluid from nasal swabs and bronchoalveolar lavage (BAL) two and four days after

201   challenge (**Fig 4a**). In unimmunized macaques two days after challenge, there were on average

202   1.3×10^5 and 1.2×10^4 copies/mL of E gene sgRNA in the nasal swab and BAL fluids, respectively

203   (**Fig. 4b,c**). In contrast, vaccinated monkeys had undetectable levels of subgenomic envelope E

204   gene RNA in the upper and lower respiratory tract (**Fig. 4b,c**). We sampled monkeys again 2

205   days later to determine if detectable virus replication was present, but again found no detectable

206   E gene sgRNA in any monkey BAL or nasal swab samples (**Fig. 4b,c**). Similarly, all RBD-

207   scNP-vaccinated macaques had undetectable N gene sgRNA in BAL and the nasal swab fluid,

208   except one macaque that had 234 copies/mL of N gene sgRNA detected on day 2 in nasal

209   swab fluid (**Fig. 4d,e**). Viral replication was undetectable in this macaque by the fourth day after

210   challenge (**Fig. 4d,e**). Thus, RBD-scNP-induced immunity prevented virus replication, and likely

211   provided sterilizing immunity, in the upper and lower respiratory tract in all but one macaque.

212

213   This study demonstrates that immunization with SARS-CoV-2 Spike either as a protein RBD-

214   scNP or as an mRNA-LNP elicits a cross-reactive antibody response capable of neutralizing

215   multiple SARS-related human and bat betaCoVs. These results demonstrate that SARS-CoV-2

216   vaccination with either the RBD-scNP or the stabilized transmembrane spike mRNA-LNP

217   vaccines currently approved for use in humans, will likely elicit cross-neutralizing antibodies with

218   the potential to prevent future animal CoV spillover events to humans [30,42,45]. The ~one log

219   higher neutralization titers induced by RBD-scNP suggests improved durability of responses.

220

221   The identification of betaCoV cross-neutralizing antibodies such as DH1047 have shown that

222   the SARS-CoV-2 RBD contains a conserved betaCoV group 2b cross-neutralizing

223   epitope[13,23,24,46,47]. Vaccination of macaques in this study showed that cross-neutralizing

224   epitopes on RBD can be potently targeted by primates. A recent study reported mosaic RBD

225   nanoparticles arrayed with RBDs from various CoVs induced cross-neutralizing antibodies in

226   mice [30]. Here, we show that cross-neutralizing antibodies are not only elicited by RBD

227   nanoparticles, but also by mRNA-LNPs expressing SARS-CoV-2 stabilized spike of the design

228   currently in mRNA COVID-19 vaccines. The 24-mer RBD-scNP nanoparticle protein adjuvanted

229   with a toll-like receptor agonist 3M-052 adsorbed to alum elicited the highest group 2b cross-

230   neutralizing antibody titers. 3M-052 formulated with alum or in an emulsion has induced long-

231   lasting memory B cells and protection against SHIV challenge in non-human primates[48,49]. A

232   Phase I clinical study using 3M-052/Alum to induce neutralizing antibody responses to an HIV

233   vaccine candidate is underway (NCT04177355). Thus, this vaccine modality represents a

234   promising first-generation pan-group 2b betaCoV vaccine with the potential to durably inhibit

235   future zoonotic transmission [25].

236

237   The emergence of SARS-CoV-2 neutralization-resistant and highly infectious variants continues

238   to be a concern for vaccine efficacy. We found here that protein nanoparticle or mRNA-LNP

239   SARS-CoV-2 spike immunization elicited SARS-CoV-2 neutralizing antibodies capable of

240   neutralizing the predominant SARS-CoV-2 variant D614G as well as the newly-emerged B.1.1.7

241 UK variant. Thus, while the B.1.1.7 variant may be more transmissible, it was equally as

242 sensitive to vaccine-induced serum neutralization as the predominant circulating SARS-CoV-2

243 D614G strain. Importantly, cross-reactive RBD-scNP immune sera and S-2P mRNA-LNP

244 immune sera bound equally as well to spike ectodomain molecules with South African B1.351,

245 Brazilian P.1 and UK B.1.1.7 RBD mutations, and are compatible with the recent demonstration

246 that current COVID-19 vaccines have efficacy, albeit reduced, against the UK and South

247 African SARS-CoV-2 variants[50-55].

248

249 Protection against asymptomatic infection and the durability of protection remain concerns for

250 current vaccines. The RBD-scNP vaccine induced robust protective immunity for SARS-CoV-2

251 replication in the upper and lower respiratory tract. This degree of virus suppression in the upper

252 respiratory tract has not been routinely achieved with SARS-CoV-2 challenge in macaques [56,57]

253 and supports the notion of inducing SARS-CoV-2 sterilizing immunity with vaccination.

254 Additionally, the extraordinarily high neutralization titers achieved by RBD-scNP vaccination

255 bode well for an extended duration of protection. Critically, as we have had 3 coronavirus

256 epidemics in the past 20 years, there is a need to develop an effective pancoronavirus vaccine

257 prior to the next pandemic. The RBD-scNP vaccine induces neutralizing antibodies to SARS-

258 CoV-1, SARS-CoV-2, batCoV-WIV-1 and batCoV-SCH014 and represents a platform for

259 producing a pancoronavirus vaccine that could prevent, rapidly temper, or extinguish the next

260 spillover of a coronavirus into humans.

261

262 **REFERENCES**

263 1   Wang, C., Horby, P. W., Hayden, F. G. & Gao, G. F. A novel coronavirus outbreak of
264   global health concern. *Lancet* **395**, 470-473, doi:10.1016/s0140-6736(20)30185-9
265   (2020).
266 2   Zaki, A. M., van Boheemen, S., Bestebroer, T. M., Osterhaus, A. D. & Fouchier, R. A.
267   Isolation of a novel coronavirus from a man with pneumonia in Saudi Arabia. *N Engl J*
268   *Med* **367**, 1814-1820, doi:10.1056/NEJMoa1211721 (2012).

269 3   Zhong, N. S. *et al.* Epidemiology and cause of severe acute respiratory syndrome (SARS)
270   in Guangdong, People's Republic of China, in February, 2003. *Lancet* **362**, 1353-1358,
271   doi:10.1016/s0140-6736(03)14630-2 (2003).

272 4   Zhu, N. *et al.* A Novel Coronavirus from Patients with Pneumonia in China, 2019. *N Engl J*
273   *Med* **382**, 727-733, doi:10.1056/NEJMoa2001017 (2020).

274 5   Zhou, P. *et al.* A pneumonia outbreak associated with a new coronavirus of probable bat
275   origin. *Nature* **579**, 270-273, doi:10.1038/s41586-020-2012-7 (2020).

276 6   Li, W. *et al.* Bats are natural reservoirs of SARS-like coronaviruses. *Science* **310**, 676-679,
277   doi:10.1126/science.1118391 (2005).

278 7   Olival, K. J. *et al.* Host and viral traits predict zoonotic spillover from mammals. *Nature*
279   **546**, 646-650, doi:10.1038/nature22975 (2017).

280 8   Memish, Z. A. *et al.* Human infection with MERS coronavirus after exposure to infected
281   camels, Saudi Arabia, 2013. *Emerg Infect Dis* **20**, 1012-1015,
282   doi:10.3201/eid2006.140402 (2014).

283 9   Sabir, J. S. *et al.* Co-circulation of three camel coronavirus species and recombination of
284   MERS-CoVs in Saudi Arabia. *Science* **351**, 81-84, doi:10.1126/science.aac8608 (2016).

285 10   Ge, X. Y. *et al.* Isolation and characterization of a bat SARS-like coronavirus that uses the
286   ACE2 receptor. *Nature* **503**, 535-538, doi:10.1038/nature12711 (2013).

287 11   Guan, Y. *et al.* Isolation and characterization of viruses related to the SARS coronavirus
288   from animals in southern China. *Science* **302**, 276-278, doi:10.1126/science.1087139
289   (2003).

290 12   Xiao, K. *et al.* Isolation of SARS-CoV-2-related coronavirus from Malayan pangolins.
291   *Nature* **583**, 286-289, doi:10.1038/s41586-020-2313-x (2020).

292 13   Pinto, D. *et al.* Cross-neutralization of SARS-CoV-2 by a human monoclonal SARS-CoV
293   antibody. *Nature* **583**, 290-295, doi:10.1038/s41586-020-2349-y (2020).

294 14   Shi, R. *et al.* A human neutralizing antibody targets the receptor-binding site of SARS-
295   CoV-2. *Nature* **584**, 120-124, doi:10.1038/s41586-020-2381-y (2020).

296 15   Ju, B. *et al.* Human neutralizing antibodies elicited by SARS-CoV-2 infection. *Nature* **584**,
297   115-119, doi:10.1038/s41586-020-2380-z (2020).

298 16   Robbiani, D. F. *et al.* Convergent antibody responses to SARS-CoV-2 in convalescent
299   individuals. *Nature* **584**, 437-442, doi:10.1038/s41586-020-2456-9 (2020).

300 17   Zost, S. J. *et al.* Potently neutralizing and protective human antibodies against SARS-CoV-
301   2. *Nature* **584**, 443-449, doi:10.1038/s41586-020-2548-6 (2020).

302 18   Liu, L. *et al.* Potent neutralizing antibodies against multiple epitopes on SARS-CoV-2
303   spike. *Nature* **584**, 450-456, doi:10.1038/s41586-020-2571-7 (2020).

304 19   Hansen, J. *et al.* Studies in humanized mice and convalescent humans yield a SARS-CoV-
305   2 antibody cocktail. *Science* **369**, 1010-1014, doi:10.1126/science.abd0827 (2020).

306 20   Brouwer, P. J. M. *et al.* Potent neutralizing antibodies from COVID-19 patients define
307   multiple targets of vulnerability. *Science* **369**, 643-650, doi:10.1126/science.abc5902
308   (2020).

309 21   Rogers, T. F. *et al.* Isolation of potent SARS-CoV-2 neutralizing antibodies and protection
310   from disease in a small animal model. *Science* **369**, 956-963,
311   doi:10.1126/science.abc7520 (2020).

312 22 Piccoli, L. *et al.* Mapping Neutralizing and Immunodominant Sites on the SARS-CoV-2
313   Spike Receptor-Binding Domain by Structure-Guided High-Resolution Serology. *Cell* **183**,
314   1024-1042.e1021, doi:10.1016/j.cell.2020.09.037 (2020).
315 23 Wec, A. Z. *et al.* Broad neutralization of SARS-related viruses by human monoclonal
316   antibodies. *Science* **369**, 731-736, doi:10.1126/science.abc7424 (2020).
317 24 Li, D. *et al.* The functions of SARS-CoV-2 neutralizing and infection-enhancing antibodies
318   in vitro and in mice and nonhuman primates. *bioRxiv*, doi:10.1101/2020.12.31.424729
319   (2021).
320 25 Burton, D. R. & Walker, L. M. Rational Vaccine Design in the Time of COVID-19. *Cell Host*
321   *Microbe* **27**, 695-698, doi:10.1016/j.chom.2020.04.022 (2020).
322 26 López-Sagaseta, J., Malito, E., Rappuoli, R. & Bottomley, M. J. Self-assembling protein
323   nanoparticles in the design of vaccines. *Comput Struct Biotechnol J* **14**, 58-68,
324   doi:10.1016/j.csbj.2015.11.001 (2016).
325 27 Bangaru, S. *et al.* Structural analysis of full-length SARS-CoV-2 spike protein from an
326   advanced vaccine candidate. *Science* **370**, 1089-1094, doi:10.1126/science.abe1502
327   (2020).
328 28 Walls, A. C. *et al.* Elicitation of Potent Neutralizing Antibody Responses by Designed
329   Protein Nanoparticle Vaccines for SARS-CoV-2. *Cell* **183**, 1367-1382 e1317,
330   doi:10.1016/j.cell.2020.10.043 (2020).
331 29 Ma, X. *et al.* Nanoparticle Vaccines Based on the Receptor Binding Domain (RBD) and
332   Heptad Repeat (HR) of SARS-CoV-2 Elicit Robust Protective Immune Responses.
333   *Immunity* **53**, 1315-1330 e1319, doi:10.1016/j.immuni.2020.11.015 (2020).
334 30 Cohen, A. A. *et al.* Mosaic nanoparticles elicit cross-reactive immune responses to
335   zoonotic coronaviruses in mice. *Science*, doi:10.1126/science.abf6840 (2021).
336 31 Saunders, K. O. *et al.* Targeted selection of HIV-specific antibody mutations by
337   engineering B cell maturation. *Science* **366**, doi:10.1126/science.aay7199 (2019).
338 32 Rappazzo, C. G. *et al.* Broad and potent activity against SARS-like viruses by an
339   engineered human monoclonal antibody. *Science*, doi:10.1126/science.abf4830 (2021).
340 33 Fox, C. B. *et al.* Adsorption of a synthetic TLR7/8 ligand to aluminum oxyhydroxide for
341   enhanced vaccine adjuvant activity: A formulation approach. *J Control Release* **244**, 98-
342   107, doi:10.1016/j.jconrel.2016.11.011 (2016).
343 34 Korber, B. *et al.* Tracking Changes in SARS-CoV-2 Spike: Evidence that D614G Increases
344   Infectivity of the COVID-19 Virus. *Cell* **182**, 812-827.e819, doi:10.1016/j.cell.2020.06.043
345   (2020).
346 35 Baden, L. R. *et al.* Efficacy and Safety of the mRNA-1273 SARS-CoV-2 Vaccine. *N Engl J*
347   *Med*, doi:10.1056/NEJMoa2035389 (2020).
348 36 Polack, F. P. *et al.* Safety and Efficacy of the BNT162b2 mRNA Covid-19 Vaccine. *N Engl J*
349   *Med* **383**, 2603-2615, doi:10.1056/NEJMoa2034577 (2020).
350 37 Galloway, S. E. *et al.* Emergence of SARS-CoV-2 B.1.1.7 Lineage - United States,
351   December 29, 2020-January 12, 2021. *MMWR Morb Mortal Wkly Rep* **70**, 95-99,
352   doi:10.15585/mmwr.mm7003e2 (2021).
353 38 Leung, K., Shum, M. H., Leung, G. M., Lam, T. T. & Wu, J. T. Early transmissibility
354   assessment of the N501Y mutant strains of SARS-CoV-2 in the United Kingdom, October

355   to November 2020. *Euro Surveill* **26**, doi:10.2807/1560-7917.ES.2020.26.1.2002106
356   (2021).

357   39   Faria, N. R. *et al.* Genomic characterisation of an emergent SARS-CoV-2 lineage in
358   Manaus: preliminary findings. *Virological* (2021).

359   40   Lassaunière, R. *et al. SARS-CoV-2 spike mutations arising in Danish mink and their spread*
360   *to humans*, <https://files.ssi.dk/Mink-cluster-5-short-report_AFO2> (2021).

361   41   Basile, K. *et al.* Cell-based culture of SARS-CoV-2 informs infectivity and safe de-isolation
362   assessments during COVID-19. *Clin Infect Dis*, doi:10.1093/cid/ciaa1579 (2020).

363   42   Menachery, V. D., Graham, R. L. & Baric, R. S. Jumping species-a mechanism for
364   coronavirus persistence and survival. *Curr Opin Virol* **23**, 1-7,
365   doi:10.1016/j.coviro.2017.01.002 (2017).

366   43   Menachery, V. D. *et al.* A SARS-like cluster of circulating bat coronaviruses shows
367   potential for human emergence. *Nat Med* **21**, 1508-1513, doi:10.1038/nm.3985 (2015).

368   44   Menachery, V. D. *et al.* SARS-like WIV1-CoV poised for human emergence. *Proc Natl*
369   *Acad Sci U S A* **113**, 3048-3053, doi:10.1073/pnas.1517719113 (2016).

370   45   Cui, J., Li, F. & Shi, Z. L. Origin and evolution of pathogenic coronaviruses. *Nat Rev*
371   *Microbiol* **17**, 181-192, doi:10.1038/s41579-018-0118-9 (2019).

372   46   Liu, H. *et al.* Cross-Neutralization of a SARS-CoV-2 Antibody to a Functionally Conserved
373   Site Is Mediated by Avidity. *Immunity* **53**, 1272-1280 e1275,
374   doi:10.1016/j.immuni.2020.10.023 (2020).

375   47   Wang, C. *et al.* A human monoclonal antibody blocking SARS-CoV-2 infection. *Nat*
376   *Commun* **11**, 2251, doi:10.1038/s41467-020-16256-y (2020).

377   48   Arunachalam, P. S. *et al.* T cell-inducing vaccine durably prevents mucosal SHIV infection
378   even with lower neutralizing antibody titers. *Nat Med* **26**, 932-940, doi:10.1038/s41591-
379   020-0858-8 (2020).

380   49   Petitdemange, C. *et al.* Vaccine induction of antibodies and tissue-resident CD8+ T cells
381   enhances protection against mucosal SHIV-infection in young macaques. *JCI Insight* **4**,
382   doi:10.1172/jci.insight.126047 (2019).

383   50   Muik, A. *et al.* Neutralization of SARS-CoV-2 lineage B.1.1.7 pseudovirus by BNT162b2
384   vaccine-elicited human sera. *Science*, doi:10.1126/science.abg6105 (2021).

385   51   Wu, K. *et al.* mRNA-1273 vaccine induces neutralizing antibodies against spike mutants
386   from global SARS-CoV-2 variants. *bioRxiv*, doi:10.1101/2021.01.25.427948 (2021).

387   52   Cele, S. *et al.* Escape of SARS-CoV-2 501Y.V2 variants from neutralization by
388   convalescent plasma. *medRxiv*, 2021.2001.2026.21250224,
389   doi:10.1101/2021.01.26.21250224 (2021).

390   53   Collier, D. *et al.* Impact of SARS-CoV-2 B.1.1.7 Spike variant on neutralisation potency of
391   sera from individuals vaccinated with Pfizer vaccine BNT162b2. *medRxiv*,
392   2021.2001.2019.21249840, doi:10.1101/2021.01.19.21249840 (2021).

393   54   Wang, Z. *et al.* mRNA vaccine-elicited antibodies to SARS-CoV-2 and circulating variants.
394   *bioRxiv*, 2021.2001.2015.426911, doi:10.1101/2021.01.15.426911 (2021).

395   55   Wibmer, C. K. *et al.* SARS-CoV-2 501Y.V2 escapes neutralization by South African COVID-
396   19 donor plasma. *bioRxiv*, 2021.2001.2018.427166, doi:10.1101/2021.01.18.427166
397   (2021).

398 56   Yu, J. *et al.* DNA vaccine protection against SARS-CoV-2 in rhesus macaques. *Science* **369**,
399   806-811, doi:10.1126/science.abc6284 (2020).
400 57   Mercado, N. B. *et al.* Single-shot Ad26 vaccine protects against SARS-CoV-2 in rhesus
401   macaques. *Nature* **586**, 583-588, doi:10.1038/s41586-020-2607-z (2020).
402 58   Laczko, D. *et al.* A Single Immunization with Nucleoside-Modified mRNA Vaccines Elicits
403   Strong Cellular and Humoral Immune Responses against SARS-CoV-2 in Mice. *Immunity*
404   **53**, 724-732 e727, doi:10.1016/j.immuni.2020.07.019 (2020).
405 59   Pardi, N. *et al.* Zika virus protection by a single low-dose nucleoside-modified mRNA
406   vaccination. *Nature* **543**, 248-251, doi:10.1038/nature21428 (2017).
407 60   Wrapp, D. *et al.* Cryo-EM structure of the 2019-nCoV spike in the prefusion
408   conformation. *Science* **367**, 1260-1263, doi:10.1126/science.abb2507 (2020).
409 61   Hsieh, C. L. *et al.* Structure-based Design of Prefusion-stabilized SARS-CoV-2 Spikes.
410   *bioRxiv*, doi:10.1101/2020.05.30.125484 (2020).
411 62   Zhou, T. *et al.* Structure-Based Design with Tag-Based Purification and In-Process
412   Biotinylation Enable Streamlined Development of SARS-CoV-2 Spike Molecular Probes.
413   *Cell Rep* **33**, 108322, doi:10.1016/j.celrep.2020.108322 (2020).
414 63   Naldini, L., Blömer, U., Gage, F. H., Trono, D. & Verma, I. M. Efficient transfer,
415   integration, and sustained long-term expression of the transgene in adult rat brains
416   injected with a lentiviral vector. *Proc Natl Acad Sci U S A* **93**, 11382-11388,
417   doi:10.1073/pnas.93.21.11382 (1996).
418 64   Yount, B. *et al.* Reverse genetics with a full-length infectious cDNA of severe acute
419   respiratory syndrome coronavirus. *Proc Natl Acad Sci U S A* **100**, 12995-13000,
420   doi:10.1073/pnas.1735582100 (2003).
421 65   Scobey, T. *et al.* Reverse genetics with a full-length infectious cDNA of the Middle East
422   respiratory syndrome coronavirus. *Proc Natl Acad Sci U S A* **110**, 16157-16162,
423   doi:10.1073/pnas.1311542110 (2013).
424 66   Hou, Y. J. *et al.* SARS-CoV-2 Reverse Genetics Reveals a Variable Infection Gradient in the
425   Respiratory Tract. *Cell* **182**, 429-446 e414, doi:10.1016/j.cell.2020.05.042 (2020).
426 67   Edgar, R. C. Search and clustering orders of magnitude faster than BLAST. *Bioinformatics*
427   **26**, 2460-2461, doi:10.1093/bioinformatics/btq461 (2010).
428 68   Nakamura, T., Yamada, K. D., Tomii, K. & Katoh, K. Parallelization of MAFFT for large-
429   scale multiple sequence alignments. *Bioinformatics* **34**, 2490-2492,
430   doi:10.1093/bioinformatics/bty121 (2018).
431 69   Valdar, W. S. Scoring residue conservation. *Proteins* **48**, 227-241,
432   doi:10.1002/prot.10146 (2002).
433
434

435 **METHODS**

436 **Animals and immunizations.** Rhesus and cynomolgus macaques were housed and treated in

437 AAALAC-accredited institutions. The study protocol and all veterinarian procedures were

438   approved by the Bioqual IACUC per a memorandum of understanding with the Duke IACUC,

439   and were performed based on standard operating procedures. Nucleoside-modified messenger

440   RNA encapsulated in lipid nanoparticles (mRNA-LNP) was prepared as previously stated [58,59].

441   Rhesus macaques (n=8) were immunized intramuscularly with 50µg of mRNA-LNP encoding

442   the receptor binding domain monomer. Cynomolgus macaques (n=5) were immunized with

443   either 50µg of mRNA-LNP encoding the transmembrane Spike protein stabilized with K986P

444   and V987P mutations. An additional group of cynomolgus macaques (n=5) were immunized in

445   the quadriceps with 100 µg of RBD-scNP adjuvanted with 5 µg of 3M-052 formulated in alum[33].

446   Biospecimens before challenge, 2 days post-challenge, and 4 days post challenge were

447   collected as described previously [24].

448   **SARS-CoV-2 intranasal and intratracheal challenge.** All animals were challenged at week 11

449   (3 weeks after last vaccination) through combined intratracheal (IT, 3.0 mL) and intranasal (IN,

450   0.5 mL per nostril) inoculation with an infectious dose of 105 PFU of SARS-CoV-2 (2019-

451   nCoV/USA-WA1/2020). The stock was generated at BIOQUAL (lot# 030120-1030, 3.31×10^5

452   PFU/mL) from a p4 seed stock obtained from BEI Resources (NR-52281). The stock underwent

453   deep sequencing to confirm homology with the WA1/2020 isolate. Virus was stored at $-80°C$

454   prior to use, thawed by hand and placed immediately on wet ice. Stock was diluted to 2.5×10^4

455   PFU/mL in PBS and vortexed gently for 5 seconds prior to inoculation. Nasal swabs,

456   bronchoalveolar lavage (BAL), plasma, and serum samples were collected seven days before,

457   two days after, and four days after challenge. Unimmunized macaques (n=50 were used as a

458   negative control group. Protection from SARS-CoV-2 infection was determined by quantitative

459   PCR of SARS-CoV-2 subgenomic envelope (E) and the more sensitive nucleocapsid (N) RNA

460   (E or N sgRNA) [39] as stated below.

461   **SARS-CoV-2 protein production.** The CoV ectodomain constructs were produce and purified

462   as describe previously [60]. The Spike (S) ectodomain was stabilized by the introduction of 2

463   prolines at amino acid positions 986 and 987 and referred to as S-2P. Plasmids encoding Spike-

464   2P and HexaPro [61] were transiently transfected in FreeStyle 293 cells (Thermo Fisher) using

465   Turbo293 (SpeedBiosystems) or 293Fectin (ThermoFisher). The constructs contained an HRV

466   3C-cleavable C-terminal twinStrepTagII-8xHis tag. On day 6, cell-free culture supernatant was

467   generated by centrifugation of the culture and filtering through a 0.8 um filter. Protein was

468   purified from filtered cell culture supernatants by StrepTactin resin (IBA) and by size exclusion

469   chromatography using Superose 6 column (GE Healthcare) in 10 mM Tris pH8,150 mM NaCl or

470   2 mM Tris pH 8, 200 mM NaCl, 0.02% NaN$_3$. ACE-2-Fc was expressed by transient transfection

471   of Freestyle 293-F cells[60]. ACE2-Fc was purified from cell culture supernatant by HiTrap protein

472   A column chromatography and Superdex200 size exclusion chromatography in 10 mM Tris

473   pH8,150 mM NaCl. SARS-CoV-2 NTD was produced as previously described [62]. SARS-CoV-2

474   fusion peptide was synthesized (GenScript).

475   **Sortase A conjugation of SARS-CoV-2 RBD to *H. pylori* ferritin nanoparticles.** Wuhan

476   strain SARS-CoV-2 RBD was expressed with sortase A donor sequence LPETGG encoded at

477   its c-terminus. C-terminal to the sortase A donor sequence was an HRV-3C cleavage site, 8X

478   his tag, and a twin StrepTagII (IBA). The SARS-CoV-2 RBD was expressed in Freestyle293

479   cells and purified by StrepTactin affinity chromatography (IBA) and superdex200 size exclusion

480   chromatography as stated above. *H. pylori* ferritin particles were expressed with a pentaglycine

481   sortase A acceptor sequence encoded at its N-terminus of each subunit. For affinity purification

482   of ferritin particles, 6XHis tags were appended C-terminal to a HRV3C cleavage site. Ferritin

483   particles with a sortase A N-terminal tag were buffer exchanged into 50mM Tris, 150mM NaCl,

484   5mM CaCI2, pH7.5. 180 µM SARS-CoV-2 RBD was mixed with 120 µM of ferritin subunits and

485   incubated with 100 µM of sortase A overnight at room temperature. Following incubation

486   conjugated particles were isolated from free ferritin or free RBD by size exclusion

487   chromatography using a Superose6 16/60 column.

488   **Biolayer interferometry binding assays.** Binding was measured using an OctetRed 96

489   (ForteBio). Anti-human IgG capture (AHC) sensor tips (Forte Bio) were hydrated for at least 10

490   minutes in PBS. ACE2 and monoclonal antibodies were diluted to 20 µg/mL in PBS and placed

491   in black 96-well assay plate. The influenza antibody CH65 was used as the background

492   reference antibody. The RBD nanoparticle was diluted to 50 µg/mL in PBS and added to the

493   assay plate. Sensor tips were loaded with antibody for 120 s. Subsequently, the sensor tips

494   were washed for 60 s in PBS to removed unbound antibody. The sensor tips were incubated in

495   a fresh well of PBS to establish baseline reading before being dipped into RBD-scNP to allow

496   association for 400 s. To measure dissociation of the antibody-RBD-scNP complex, the tip was

497   incubated in PBS for 600 s. At the end of dissociation, the tip was ejected and a new tip was

498   attached to load another antibody. The data was analyzed with Data Analysis HT v12

499   (ForteBio). Background binding observed with CH65 was subtracted from all values. All binding

500   curves were aligned to the start of association. The binding response at the end of the 400 s

501   association phase was plotted in GraphPad Prism v9.0.

502   **Surface plasmon resonance (SPR) assays.** SPR measurements of DH1047 antigen binding

503   fragment (Fab) binding to monomeric SARS-CoV-2 receptor binding domain (RBD) proteins

504   were performed in HBS-EP+ running buffer using a Biacore S200 instrument (Cytiva). Assays

505   were performed in the DHVI BIA Core Facility. The RBD was first captured via its twin-

506   StrepTagII onto a Series S Streptavidin chip to a level of 300-400 resonance units (RU). The

507   antibody Fabs were injected at 0.5 to 500 nM over the captured S proteins using the single

508   cycle kinetics injection mode at a flow rate of 50 µL/min. Fab association occurred for 180 s

509   followed by a dissociation of 360 seconds after the end of the association phase. At the end of

510   the dissociation phase the RBD was regenerated with a 30 s injection of glycine pH1.5. Binding

511   values were analyzed with Biacore S200 Evaluation software (Cytiva). References included

512   blank streptavidin surface along with blank buffer binding and was subtracted from DH1047

513   values to account for signal drift and non-specific protein binding. A 1:1 Langmuir model with a

514   local Rmax was used for curve fitting. Binding rates and constants were derived from the curve.

515   Representative results from two independent experiments are shown.

516   **SARS-CoV-2 pseudovirus neutralization.** Neutralization of SARS-CoV-2 Spike-pseudotyped

517   virus was performed by adapting an infection assay described previously with lentiviral vectors

518   and infection in 293T/ACE2.MF (the cell line was kindly provided by Drs. Mike Farzan and

519   Huihui Mu at Scripps). Cells were maintained in DMEM containing 10% FBS and 50 µg/ml

520   gentamicin. An expression plasmid encoding codon-optimized full-length spike of the Wuhan-1

521   strain (VRC7480), was provided by Drs. Barney Graham and Kizzmekia Corbett at the Vaccine

522   Research Center, National Institutes of Health (USA). The D614G mutation was introduced into

523   VRC7480 by site-directed mutagenesis using the QuikChange Lightning Site-Directed

524   Mutagenesis Kit from Agilent Technologies (Catalog # 210518). The mutation was confirmed by

525   full-length spike gene sequencing. Pseudovirions were produced in HEK 293T/17 cells (ATCC

526   cat. no. CRL-11268) by transfection using Fugene 6 (Promega, Catalog #E2692). Pseudovirions

527   for 293T/ACE2 infection were produced by co-transfection with a lentiviral backbone (pCMV

528   ΔR8.2) and firefly luciferase reporter gene (pHR' CMV Luc) [63]. Culture supernatants from

529   transfections were clarified of cells by low-speed centrifugation and filtration (0.45 µm filter) and

530   stored in 1 ml aliquots at -80 °C.

531   For 293T/ACE2 neutralization assays, a pre-titrated dose of virus was incubated with 8

532   serial 3-fold or 5-fold dilutions of mAbs in duplicate in a total volume of 150 µL for 1 hr at 37 °C

533   in 96-well flat-bottom poly-L-lysine-coated culture plates (Corning Biocoat). Cells were

534   suspended using TrypLE express enzyme solution (Thermo Fisher Scientific) and immediately

535   added to all wells (10,000 cells in 100 µL of growth medium per well). One set of 8 control wells

536   received cells + virus (virus control) and another set of 8 wells received cells only (background

537   control). After 66-72 h of incubation, medium was removed by gentle aspiration and 30 µL of

538   Promega 1x lysis buffer was added to all wells. After a 10-minute incubation at room

539   temperature, 100 µl of Bright-Glo luciferase reagent was added to all wells. After 1-2 minutes,

540   110 µl of the cell lysate was transferred to a black/white plate (Perkin-Elmer). Luminescence

541   was measured using a PerkinElmer Life Sciences, Model Victor2 luminometer. Neutralization

542   titers are the serum dilution (ID50/ID80) at which relative luminescence units (RLU) were

543   reduced by 50% and 80% compared to virus control wells after subtraction of background

544   RLUs.

545   **Plasma IgG blocking of ACE2 binding.** For ACE2 blocking assays, plates were coated with 2

546   μg/mL recombinant ACE2 protein, then washed and blocked with 3% BSA in 1X PBS. While

547   assay plates blocked, purified antibodies were diluted as stated above, only in 1% BSA with

548   0.05% Tween-20. In a separate dilution plate Spike-2P protein was mixed with the antibodies at

549   a final concentration equal to the EC50 at which spike binds to ACE2 protein. The mixture was

550   allowed to incubate at room temperature for 1 hour. Blocked assay plates were then washed

551   and the antibody-spike mixture was added to the assay plates for a period of 1 hour at room

552   temperature. Plates were washed and a polyclonal rabbit serum against the same spike protein

553   (nCoV-1 nCoV-2P.293F) was added for 1 hour, washed and detected with goat anti rabbit-HRP

554   (Abcam cat# ab97080) followed by TMB substrate. The extent to which antibodies were able to

555   block the binding spike protein to ACE2 was determined by comparing the OD of antibody

556   samples at 450 nm to the OD of samples containing spike protein only with no antibody. The

557   following formula was used to calculate percent blocking: blocking% = (100 - (OD sample/OD of

558   spike only)*100).

559   **Plasma IgG blocking of RBD monoclonal antibody binding.** Blocking assays for DH1041

560   and DH1047 were performed as stated above for ACE2, except plates were coated with either

561   DH1041 or DH1047 instead of ACE2.

562   **Plasma IgG ELISA binding assays.** For ELISA binding assays of Coronavirus Spike

563   antibodies, the antigen panel included SARS-CoV-2 Spike S1+S2 ectodomain (ECD) (SINO,

564   Catalog # 40589-V08B1), SARS-CoV-2 Spike-2P [60], SARS-CoV-2 Spike S2 ECD (SINO,

565   Catalog # 40590-V08B), SARS-CoV-2 Spike RBD from insect cell sf9 (SINO, Catalog # 40592-

566   V08B), SARS-CoV-2 Spike RBD from mammalian cell 293 (SINO, Catalog # 40592- V08H),

567   SARS-CoV-2 Spike NTD-Biotin, SARS-CoV Spike Protein DeltaTM (BEI, Catalog # NR-722),

568   SARS-CoV WH20 Spike RBD (SINO, Catalog # 40150-V08B2), SARS-CoV WH20 Spike S1

569   (SINO, Catalog #40150-V08B1), SARS-CoV-1 RBD, MERS-CoV Spike S1+S2 (SINO, Catalog

570   # 40069-V08B), MERS-CoV Spike S1 (SINO, Catalog #40069-V08B1), MERS-CoV Spike S2

571   (SINO, Catalog #40070-V08B), MERS-CoV Spike RBD (SINO, Catalog #40071-V08B1), MERS-

572   CoV Spike RBD.

573   For binding ELISA, 384-well ELISA plates were coated with 2 μg/mL of antigens in 0.1 M

574   sodium bicarbonate overnight at 4°C. Plates were washed with PBS + 0.05% Tween 20 and

575   blocked with assay diluent (PBS containing 4% (w/v) whey protein, 15% Normal Goat Serum,

576   0.5% Tween-20, and 0.05% Sodium Azide) at room temperature for 1 hour. Purified mAb

577   samples in 3-fold serial dilutions in assay diluent starting at 100 μg/mL were added and

578   incubated for 1 h, followed by washes with PBS-0.1% Tween 20. HRP-conjugated goat anti-

579   human IgG secondary Ab (SouthernBiotech, catalog #2040-05) was diluted to 1:10,000 and

580   incubated at room temperature for 1 hour. These plates were washed four times and developed

581   with tetramethylbenzidine substrate (SureBlue Reserve- KPL). The reaction was stopped with 1

582   M HCl, and optical density at 450 nm (OD_{450}) was determined.

583   **Subgenomic RNA real time PCR quantification.** The assay for SARS-CoV-2 quantitative

584   Polymerase Chain Reaction (qPCR) detects total RNA using the WHO primer/probe set

585   E_Sarbeco (Charité/Berlin). A QIAsymphony SP (Qiagen, Hilden, Germany) automated sample

586   preparation platform along with a virus/pathogen DSP midi kit and the *complex800* protocol

587   were used to extract viral RNA from 800 μL of pooled samples. A reverse primer specific to the

588   envelope gene of SARS-CoV-2 (5'-ATA TTG CAG CAG TAC GCA CAC A-3') was annealed to

589   the extracted RNA and then reverse transcribed into cDNA using SuperScript™ III Reverse

590   Transcriptase (Thermo Fisher Scientific, Waltham, MA) along with RNAse Out (Thermo Fisher

591   Scientific, Waltham, MA). The resulting cDNA was treated with RNase H (Thermo Fisher

592   Scientific, Waltham, MA) and then added to a custom 4x TaqMan™ Gene Expression Master

593 Mix (Thermo Fisher Scientific, Waltham, MA) containing primers and a fluorescently labeled

594 hydrolysis probe specific for the envelope gene of SARS-CoV-2 (forward primer 5'-ACA GGT

595 ACG TTA ATA GTT AAT AGC GT-3', reverse primer 5'-ATA TTG CAG CAG TAC GCA CAC A-

596 3', probe 5'-6FAM/AC ACT AGC C/ZEN/A TCC TTA CTG CGC TTC G/IABkFQ-3'). The qPCR

597 was carried out on a QuantStudio 3 Real-Time PCR System (Thermo Fisher Scientific,

598 Waltham, MA) using the following thermal cycler parameters: heat to 50°C, hold for 2 min, heat

599 to 95°C, hold for 10 min, then the following parameters are repeated for 50 cycles: heat to 95°C,

600 hold for 15 seconds, cool to 60°C and hold for 1 minute. SARS-CoV-2 RNA copies per reaction

601 were interpolated using quantification cycle data and a serial dilution of a highly characterized

602 custom DNA plasmid containing the SARS-CoV-2 envelope gene sequence. Mean RNA copies

603 per milliliter were then calculated by applying the assay dilution factor (DF=11.7). The limit of

604 detection (LOD) for this assay is approximately 62 RNA copies per mL of sample.

605 **Live virus neutralization assays.** Full-length SARS-CoV-2, SARS-CoV, WIV-1, and

606 RsSHC014 viruses were designed to express nanoluciferase (nLuc) and were recovered via

607 reverse genetics as described previously [64-66]. Virus titers were measured in Vero E6 USAMRIID

608 cells, as defined by plaque forming units (PFU) per ml, in a 6-well plate format in quadruplicate

609 biological replicates for accuracy. For the 96-well neutralization assay, Vero E6 USAMRID cells

610 were plated at 20,000 cells per well the day prior in clear bottom black walled plates. Cells were

611 inspected to ensure confluency on the day of assay. Serum samples were tested at a starting

612 dilution of 1:20 and were serially diluted 3-fold up to nine dilution spots. Serially diluted serum

613 samples were mixed in equal volume with diluted virus. Antibody-virus and virus only mixtures

614 were then incubated at 37°C with 5% CO_2 for one hour. Following incubation, serially diluted

615 sera and virus only controls were added in duplicate to the cells at 75 PFU at 37°C with 5%

616 CO_2. After 24 hours, cells were lysed, and luciferase activity was measured via Nano-Glo

617 Luciferase Assay System (Promega) according to the manufacturer specifications.

618 Luminescence was measured by a Spectramax M3 plate reader (Molecular Devices, San Jose,

619   CA). Virus neutralization titers were defined as the sample dilution at which a 50% reduction in

620   RLU was observed relative to the average of the virus control wells.

621   **Biocontainment and biosafety.** All work described here was performed with approved

622   standard operating procedures for SARS-CoV-2 in a biosafety level 3 (BSL-3) facility

623   conforming to requirements recommended in the Microbiological and Biomedical Laboratories,

624   by the U.S. Department of Health and Human Service, the U.S. Public Health Service, and the

625   U.S. Center for Disease Control and Prevention (CDC), and the National Institutes of Health

626   (NIH).

627   **Recombinant IgG production.** Expi293-F cells were diluted to 2.5E6 cells/mL on the day of

628   transfection. Cells were co-transfected with Expifectamine and heavy and light chain expression

629   plasmids. Enhancers were added 16h after transfection. On day 5, the cell culture was cleared

630   of cells by centrifugation, filtered, and incubated with protein A beads overnight. The next day

631   the protein A resin was washed with Tris buffered saline and then added to a 25 mL column.

632   The resin was washed again and then glacial acetic acid was used to elute antibody off of the

633   protein A resin. The pH of the solution was neutralized with 1M Tris pH8. The antibody was

634   buffer exchanged into 25 mM sodium citrate pH6 supplemented with 150 mM NaCl, 0.2 μm

635   filtered, and frozen at -80°C.

636   **Negative stain electron microscopy.** The RBD nanoparticle protein at ~1-5 mg/ml

637   concentration that had been flash frozen and stored at -80 °C was thawed in an aluminum block

638   at 37 °C for 5 minutes; then 1-4 μL of RBD nanoparticle was diluted to a final concentration of

639   0.1 mg/ml into room-temperature buffer containing 150 mM NaCl, 20 mM HEPES pH 7.4, 5%

640   glycerol, and 7.5 mM glutaraldehyde. After 5 minutes cross-linking, excess glutaraldehyde was

641   quenched by adding sufficient 1 M Tris pH 7.4 stock to give a final concentration of 75 mM Tris

642   and incubated for 5 minutes. For negative stain, carbon-coated grids (EMS, CF300-cu-UL) were

643   glow-discharged for 20s at 15 mA, after which a 5-μl drop of quenched sample was incubated

644   on the grid for 10-15 s, blotted, and then stained with 2% uranyl formate. After air drying grids

645   were imaged with a Philips EM420 electron microscope operated at 120 kV, at

646   82,000× magnification and images captured with a 2k x 2k CCD camera at a pixel size of 4.02

647   Å.

648   **Processing of negative stain images.** The RELION 3.0 program was used for all negative

649   stain image processing. Images were imported, CTF-corrected with CTFFIND, and particles

650   were picked using a spike template from previous 2D class averages of spike alone. Extracted

651   particle stacks were subjected to 2-3 rounds of 2D class averaging and selection to discard junk

652   particles and background picks. Cleaned particle stacks were then subjected to 3D classification

653   using a starting model created from a bare spike model, PDB 6vsb, low-pass filtered to 30 Å.

654   Classes that showed clearly-defined Fabs were selected for final refinements followed by

655   automatic filtering and B-factor sharpening with the default Relion post-processing parameters.

656   **Betacoronavirus sequence analysis.** Heatmaps of amino acid sequence similarity were

657   computed for a representative set of betacoronaviruses using the ComplexHeatmap package in

658   R. Briefly, 1408 betacoronavirus sequences were retrieved from NCBI Genbank, aligned to the

659   Wuhan-1 spike protein sequence, and trimmed to the aligned region. The 1408 spike

660   sequences were then clustered using USEARCH [67] with a sequence identity threshold of 0.90

661   resulting in 52 clusters. We sampled one sequence from each cluster to generate a

662   representative set of sequences. Five betacoronavirus sequences of interest not originally

663   included in the clustered set were added: SARS-CoV-2, GXP4L, batCoV-RaTG13, batCoV-

664   SHC014, batCoV-WIV-1. This resulted in a set of 57 representative spike sequences. Pairs of

665   spike amino acid sequences were aligned using a global alignment and the BLOSUM62 scoring

666   matrix. For RBD and NTD domain alignments, spike sequences were aligned to the Wuhan 1

667   spike protein RBD region (residues 330-521) and NTD region (residues 27-292), respectively,

668   and trimmed to the aligned region. Phylogenetic tree construction of RBD sequences was

669   performed with Geneious Prime 2020.1.2 using the Neighbor Joining method and default

670   parameters. To map group 2b betaCoV sequence conservation onto the RBD structure, group

671   2b spike sequences were retrieved from Genbank and clustered using USEARCH [67] with a

672   sequence identity threshold of 0.99 resulting in 39 clusters. For clusters of size >5, 5 spike

673   sequences were randomly downsampled from each cluster. The resulting set of 73 sequences

674   was aligned using MAFFT [68]. Conservation scores for each position in the multiple sequence

675   alignment were calculated using the trident scoring method [69] and computed using the MstatX

676   program (https://github.com/gcollet/MstatX). The conservation scores were then mapped to the

677   RBD domain coordinates (PDB: 7LD1) and images rendered with PyMol version 2.3.5.

678   **Statistics Analysis.** Data were plotted using Prism GraphPad 8.0. Wilcoxon rank sum exact

679   test was performed to compare differences between groups with p-value < 0.05 considered

680   significant using SAS 9.4 (SAS Institute, Cary, NC). No adjustments were made to the p-values

681   for multiple comparisons. IC50 and IC80 values were calculated using R statistical software

682   (version 4.0.0; R Foundation for Statistical Computing, Vienna, Austria). The R package 'nplr'

683   was used to fit 4-Parameter Logistic (4-PL) regression curves to the average values from

684   duplicate experiments, and these fits were used to estimate the concentrations corresponding to

685   50% and 80% neutralization.

686

708

709   **AUTHOR CONTRIBUTIONS**

710   KOS and BFH designed and managed the study, reviewed all data and wrote and edited the

711   manuscript; DW, NP designed and produced the mRNA-LNPs; EL, AMS, FPC, and HC

712   expressed proteins; EL, RP, MB, THO, DRM, DCM, LVT, TDS, RSB carried out binding or

713   neutralization assays; RSB and DRM prepared recombinant live viruses encoding nLuc; DL,

714   CTM, TD, MG, DCD designed or performed sg or genomic RNA assays; RJE, SG, PA, KatM,

715   KarM, MA, MB, and KW performed structural or sequence analysis; SMA performed SPR; LLS,

716   MGL, HA, RS and IM performed or evaluated monkey studies; CWW, EWP, GDS collected,

717   annotated, COVID-19 samples; MT selected, provided adjuvant; RWR and RLS performed

718   statistical analyses; All authors edited and approved the manuscript.

719

720   **Supplementary information is available for this paper**

721   **Correspondence** and requests for materials should be addressed to

722   kevin.saunders@duke.edu and barton.haynes@duke.edu

723

724 **Reprints and permissions information is available at www.nature.com/reprints**

725 **Competing financial interests** MAT is an employee of 3M Company. 3M company had no role

726 in the execution of the study, data collection, or data interpretation. BFH, KOS, and MAT have

727 filed patents regarding the nanoparticle vaccine. DW is named on patents that describe the use

728 of nucleoside-modified mRNA as a platform to deliver therapeutic proteins. DW and NP are also

729 named on a patent describing the use of nucleoside-modified mRNA in lipid nanoparticles as a

730 vaccine platform. All other authors declare no competing interests.

731

732 **FIGURE LEGENDS**

733 **Figure 1. SARS-CoV-2 receptor binding domain (RBD) sortase conjugated nanoparticles**

734 **(scNPs) elicits extremely high titers of SARS-CoV-2 pseudovirus neutralizing antibodies.**

735 **a.** SARS-CoV-2 RBD nanoparticles were constructed by expressing RBD with a C-terminal

736 sortase A donor sequence (blue and red) and a *Helicobacter pylori* ferritin nanoparticle with N-

737 terminal sortase A acceptor sequences (gray) on each subunit (top left). The RBD is shown in

738 blue with the ACE2 binding site in red. The RBD was conjugated to nanoparticles by a sortase A

739 (SrtA) enzyme conjugation reaction (top right). The resultant nanoparticle is modeled on the

740 bottom left. Nine amino acid sortase linker is shown in orange. Two dimensional class averages

741 of negative stain electron microscopy images of actual RBD nanoparticles are shown on the

742 bottom right.

743 **b.** Antigenicity of RBD nanoparticles determined by biolayer interferometry against a panel of

744 SARS-CoV-2 antibodies and the ACE2 receptor. Antibodies are color-coded based on epitope

745 and function. N-terminal domain (NTD), nonAbs IE, infection enhancing non-neutralizing

746 antibody; nAb, neutralizing antibody; nonAb, non-neutralizing antibody. Mean and standard

747 error from 3 independent experiments are shown.

748   **c.** Cynomolgus macaque challenge study scheme. Blue arrows indicate RBD-NP immunization

749   timepoints. Intranasal/intratracheal SARS-CoV-2 challenge is indicated at week 10.

750   **d.** Macaque serum IgG binding determined by ELISA to recombinant SARS-CoV-2 stabilized

751   Spike ectodomain (S-2P), RBD, NTD, and Fusion peptide (FP). Binding titer is shown as area-

752   under-the curve of the $\log_{10}$-transformed curve. Arrows indicate immunization timepoints.

753   **e.** Plasma antibody blocking of SARS-CoV-2 S-2P binding to ACE2-Fc and RBD neutralizing

754   antibody DH1041. Group mean and standard error are shown.

755   **f.** Dose-dependent serum neutralization of SARS-COV-2 pseudotyped virus infection of ACE2-

756   expressing 293T cells. Serum was collected after two immunizations. The SARS-CoV-2

757   pseudovirus spike has an aspartic acid to glycine change at position 614 (D614G). Each curve

758   represents a single macaque.

759   **g.** Heat map of serum neutralization ID50 and ID80 titers for SARS-COV-2 D614G pseudotyped

760   virus after two immunizations.

761   **h.** SARS-COV-2 D614G pseudotyped virus serum neutralization kinetics. Each curve

762   represents a single macaque.

763   **i.** Comparison of serum neutralization ID50 titers from cynomolgus macaques immunized with

764   recombinant protein RBD nanoparticles (blue) or nucleoside-modified mRNA-LNP expressing S-

765   2P (burgundy) (**$P<0.01$, Two-tailed Exact Wilcoxon test n = 5).

766   **j.** Comparison of serum neutralization titers obtained from RBD-scNP-vaccinated macaques

767   (blue) and SARS-CoV-2 infected humans (shades of green). Human samples were stratified

768   based on disease severity as asymptomatic (N=34), symptomatic (n=71), and hospitalized

769   (N=60) (**$P<0.01$, Two-tailed Wilcoxon test n = 5).

770

771   **Figure 2. RBD-scNP immunization elicits higher titers of neutralizing antibodies and**

772   **binding antibodies against more transmissible SARS-CoV-2 variants than stabilized**

773   **spike mRNA-LNP vaccination.**

774   **a**. Comparison of serum neutralization ID50 titers from cynomolgus macaques immunized with

775   recombinant protein RBD sortase conjugated nanoparticles (RBD-scNP; blue) or nucleoside-

776   modified mRNA-LNP expressing S-2P (burgundy). ID50 titers (left) and ID80 titers (right) are

777   shown. Horizontal bars are the group geometric mean (**P<0.01, Two-tailed Exact Wilcoxon

778   test n = 5).

779   **b.** Fold decrease in neutralization potency between neutralization of SARS-CoV-2 D614G and

780   SARS-CoV-2 B.1.1.7 pseudoviruses. Fold change is shown for RBD-scNP-immunized and

781   mRNA-LNP-immunized macaques based ID50 (left) and ID80 (right) titers. Horizontal bars are

782   the group mean.

783   **c**. ACE2 receptor and cross-neutralizing antibody DH1047 ELISA binding to SARS-CoV-2 Spike

784   ectodomain (ECD) based on a Danish mink (H69/V70del/Y453F/D614G/I692V), B.1.351 or P.1-

785   like (K417N/E484K/N501Y/D614G), and B.1.1.7

786   (H69/V70del/Y144del/N501Y/A570D/D614G/P681H/T716I/S982A/D1118H) strains. Titers are

787   shown as area under the log-transformed curve (log AUC).

788   **d** RBD-scNP and S-2P mRNA-LNP-immunized macaque serum IgG ELISA binding to SARS-

789   CoV-2 Spike variants shown in **c**. Serum was tested after two immunizations. Horizontal bars

790   are the group mean.

791   **e** ACE2 receptor (gray), cross-neutralizing antibody DH1047 (navy), and ACE2 binding site-

792   targeting neutralizing antibody DH1041 (green) ELISA binding to SARS-CoV-2 Spike RBD

793   monomers. RBD variants contain mutations found in circulating B.1.351 and P.1 virus strains.

794   Titers are shown as area under the log-transformed curve (log AUC).

795   **f** RBD-scNP and S-2P mRNA-LNP-immunized macaque serum IgG ELISA binding to SARS-

796   CoV-2 Spike RBD variants shown in **e**. Serum was tested after two immunizations. Horizontal

797   bars are the group mean.

798

799 **Figure 3. RBD-scNP vaccine induction of serum cross-neutralization of SARS-related**

800 **betacoronavirus infection.**

801 **a**. Sera from macaques immunized twice with RBD-scNP, S-2P mRNA-LNP, or RBD mRNA-

802 LNP neutralize replication-competent SARS-related human (SARS-CoV-1 and SARS-CoV-2)

803 and bat (WIV-1 and SHC014) betaCoVs. Each symbol indicates the ID50 of an individual

804 macaque. Horizontal bars are the group mean (*P<0.05, **P<0.01, Two-tailed Exact Wilcoxon

805 test, n = 5 or 8).

806 **b**. Comparison of serum cross-neutralization after two (circles) or three (diamonds) RBD scNP

807 immunizations. Each symbol indicates the ID50 of an individual macaque. Horizontal bars are

808 the group mean.

809 **c**. Plasma IgG from macaques immunized twice with RBD-scNP binds to human, bat, and

810 pangolin SARS-related betacoronavirus S protein in ELISA. ECD, ectodomain.

811 **d**. Cryo-electron microscopy model comparing the epitopes of SARS-CoV-2-specific neutralizing

812 RBD antibody (DH1041) and cross-neutralizing RBD antibody (DH1047). (Left) Cartoon view of

813 Spike bound to DH1047 (magenta; PDB ID: 7LD1) fitted in the cryo-EM map (transparent gray;

814 EMD-23279). Receptor Binding Domain (RBD) is in gray, Receptor Binding Motif (RBM) is in

815 blue, and the rest of Spike is in forest green. (Top, right) Zoomed-in surface view of RBD (gray)

816 and RBM (blue) binding interface with DH1047 (magenta) compared to the neutralizing RBD

817 antibody DH1041 (red; PDB ID: 7LAA; EMD-23246). The RBDs of the two complexes from their

818 respective cryo-EM structures were overlaid for comparison. (Bottom, right) A 180° rotated view

819 of the top-right panel.

820 **e**. DH1047 epitope is conserved within group 2b betaCoVs. Receptor binding domain (surface

821 representation) colored by conservation within group 2b betacoronaviruses. DH1047 epitope is

822 shown in magenta outline.

823   **f.** Sequence similarity of RBD for representative betacoronaviruses. Heatmaps displaying

824   pairwise amino acid sequence similarity for 57 representative betacoronaviruses. Dark blue

825   shading indicates high sequence similarity.

826   **g.** Macaque plasma antibody blocking of SARS-CoV-2 and batCoV-SHC014 S-2P binding to

827   ACE2-Fc and RBD cross-neutralizing antibody DH1047. Group mean and standard error are
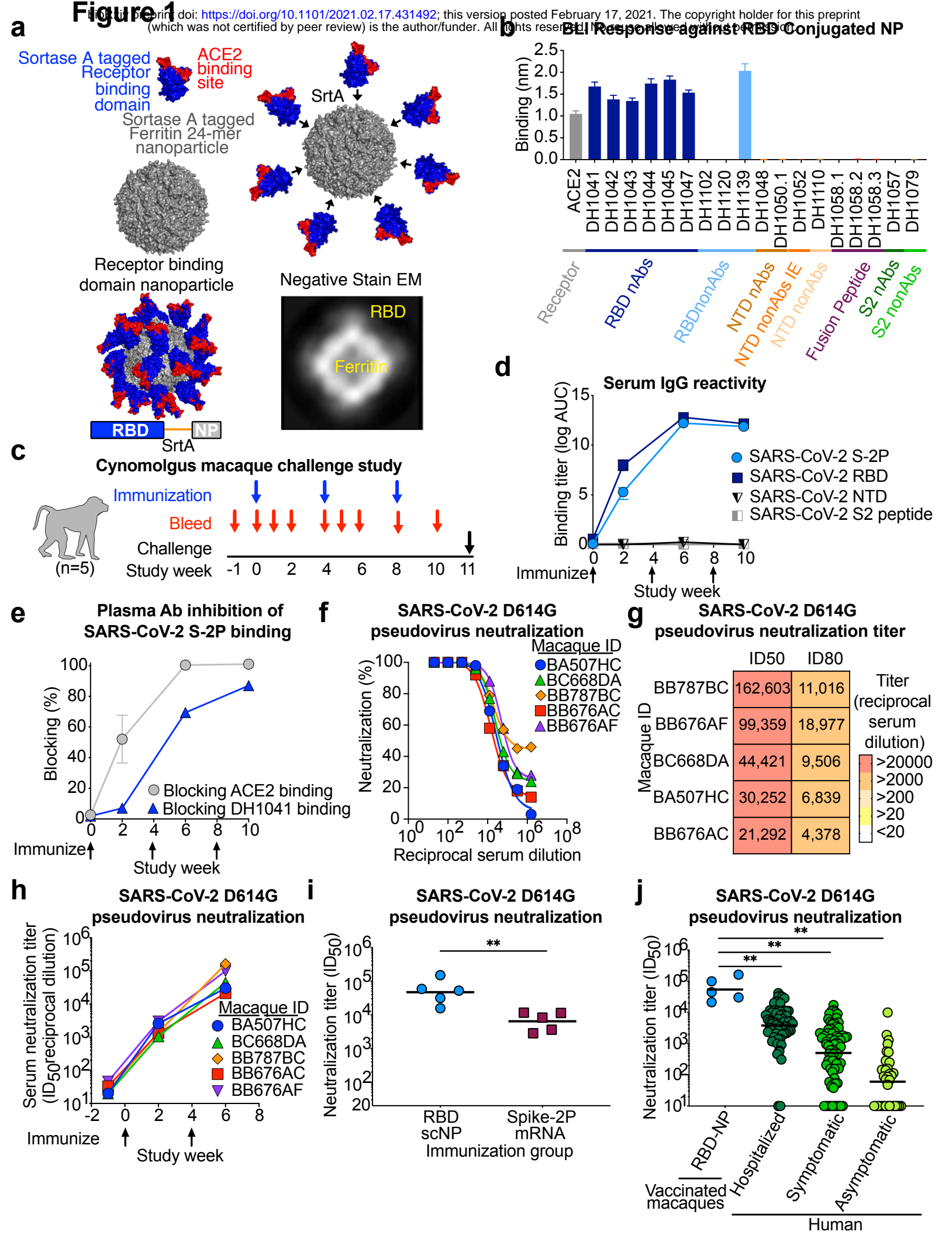
828   shown.

829   **h.** Rhesus plasma and convalescent human serum antibody blocking of SARS-CoV-2 S-2P

830   binding to ACE2-Fc and RBD cross-neutralizing antibody DH1047. Each symbol represents a

831   macaque or infected individual. Black horizontal bars indicate group mean and standard error.

832   **Figure 4. RBD-scNP vaccination completely prevents virus replication in the upper and**

833   **lower respiratory tract after intranasal and intratracheal SARS-CoV-2 challenge in all but**

834   **one macaque.**

835   **a.** Macaque intranasal/intratracheal SARS-CoV-2 challenge study design. Blue arrows indicate

836   the time points for RBD-nanoparticle immunizations. Biospecimens were collected as indicated

837   by the green and orange arrows.
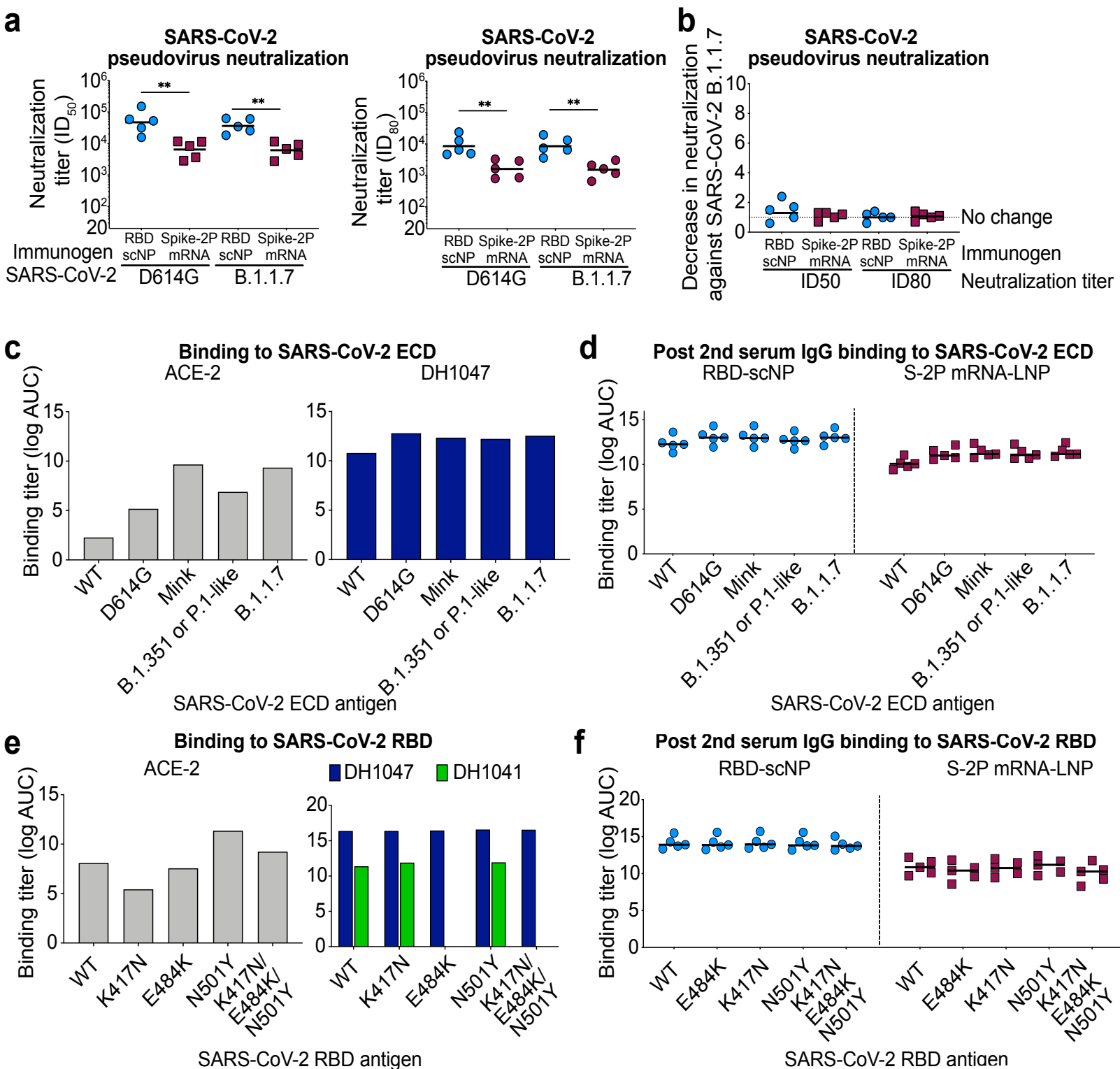
838   **b-e**. Quantification of viral subgenomic RNA (sgRNA) in unimmunized (gray symbols) and RBD-

839   scNP-immunized (red or blue symbols) macaques. sgRNA encoding the **b, c** envelope (E) gene

840   or **d, e** nucleocapsid (N) gene of SARS-CoV-2 was quantified two (left) and four (right) days

841   after SARS-CoV-2 challenge. E or N gene sgRNA was measured in both **b, d** nasal swabs and

842   **c, e** bronchoalveolar lavage (BAL) fluids from each macaque. Limit of detection (LOD) for the

843   assay is 150 copies/mL. Each symbol represents an individual macaque with the group mean

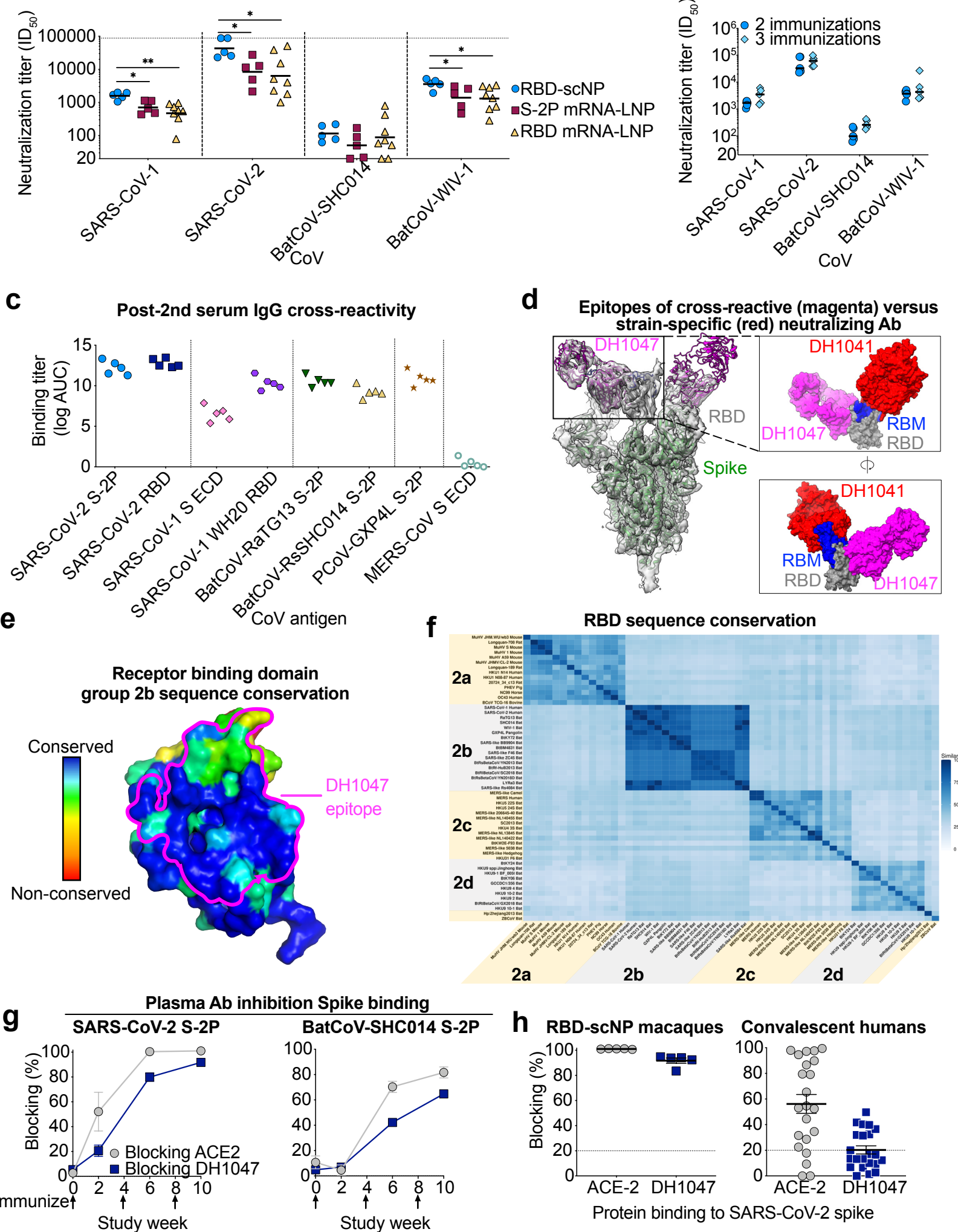844   shown with a horizontal bar (**P<0.01, Two-tailed Exact Wilcoxon test n = 5).

Figure 1

Figure 2

Figure 3

a NHP serum CoV neutralization

b Macaque serum CoV neutralization

c Post-2nd serum IgG cross-reactivity

d Epitopes of cross-reactive (magenta) versus strain-specific (red) neutralizing Ab

e Receptor binding domain group 2b sequence conservation

f RBD sequence conservation

g Plasma Ab inhibition Spike binding

h RBD-scNP macaques / Convalescent humans

Figure 4

a Cynomolgus macaque challenge study

b Envelope (E) sgRNA

d Nucleocapsid (N) sgRNA